

Pressure-Induced Phase Transitions in *trans*-Stilbene Crystals

Hideyoshi Takeshita, Yoshio Suzuki,[1] Yuko Hirai, Yoshinori Nibu, Hiroko Shimada,* and Ryoichi Shimada[1]

Department of Chemistry, Faculty of Science, Fukuoka University, Nanakuma, Jonan-ku, Fukuoka 814-0180

[1]Department of Information Electronics, Faculty of Engineering, Fukuoka Institute of Technology, Wajiro-Higashi, Higashi-ku, Fukuoka 811-0214

Received May 20, 2003; E-mail: shimada@fukuoka-u.ac.jp

Pressure effects on the phase transitions in [$^1H_{12}$] and [$^2H_{12}$]*trans*-stilbene crystals were studied. Pressure–frequency plots and pressure–half band width plots for the Raman bands due to the inter- and intramolecular vibrations of [$^1H_{12}$] and [$^2H_{12}$]*trans*-stilbene crystals showed inflectional variations of the slopes of the plots at about 2 and 4 GPa. The fact that no clear discontinuous changes of the slopes of the plots were observed indicates that the second-order phase transitions take place at about 2 and 4 GPa. The low-frequency Raman bands of [$^1H_{12}$] and [$^2H_{12}$]*trans*-stilbene crystals were reinvestigated and assignments to the intermolecular rotational vibrations about the *x*, *y*, and *z* axes were made on the basis of the isotopic effect on the vibrational frequency.

The molecular and crystal structures of [$^1H_{12}$]*trans*-stilbene (stilbene-d_0) were studied by many workers.[1–5] The molecular structure in solid is almost planar, with two phenyl rings twisted very slightly from the ethylenic plane of the molecule,[1–3] while the structure is non-planar in vapor[4] and fluid[5] phases. The crystal structure of stilbene-d_0 belongs to the monoclinic space group $P2_1/c$ with four molecules in the unit cell. The four molecules fall into two crystallographically inequivalent sites; one of these two sites shows orientational disorder. The crystal structure is highly disordered at room temperature, while orientational disorder almost disappears at 113 K and the lattice becomes more ordered.[2]

Bree and Edelson gave the assignment for the intermolecular vibrations of stilbene-d_0 crystal through polarization measurements of the low-frequency Raman bands at various temperatures between room temperature and 4.2 K.[6] Chakrabarti and Misra studied the temperature-induced phase transitions of stilbene-d_0 crystal through observation of temperature dependencies on the frequencies and band widths of the Raman bands.[7] They showed that the phase transition of order–disorder type takes place over the narrow temperature range 215–225 K. The well-established disordered structure of stilbene-d_0 crystal at room temperature attains an ordered structure at low temperature through one or two order–disorder transitions.[7] They observed a break point in the curve of the temperature–band width plots in the lower temperature region 105–115 K, but no conclusion about a phase transition could be drawn for this break point due to the wide experimental error in this region. Saito et al. measured the temperature dependence of the heat capacity for stilbene-d_0 crystal.[8] They could not find any discontinuous changes of the heat capacity at 215–225 K or at 105–115 K, but they found an anomalous behavior of the temperature–heat capacity plots at about 170 K. Thus they concluded that the glass transition attributed to the freezing of the intramolecular crankshaft motion takes place at about 170 K in stilbene-d_0 crystal.[8] Saito and Ikemoto studied the lattice-dynamics for stilbene-d_0 crystal theoretically considering the incorporation of the intramolecular twisting vibration of the phenyl rings and showed that the twisting vibration of the phenyl rings strongly couples with the overall rotation of the molecule.[9]

Study of the intramolecular vibrations of stilbene-d_0 was made by various workers through observation of the Raman and infrared spectra and also through calculation of the normal vibrations.[6,10–13]

The aims of the work reported here are (1) confirmation of the occurrence of the phase transition of order–disorder type at 215–225 K (and 105–115 K)[7] and the glass transition at about 170 K,[8] and (2) observation of the pressure-induced phase transitions through the study of the Raman active inter- and intramolecular vibrations of stilbene-d_0 and [$^2H_{12}$]*trans*-stilbene (stilbene-d_{12}) crystals at various pressures and temperatures. The low-frequency Raman bands of stilbene-d_0 and -d_{12} crystals are reinvestigated on the basis of the isotopic effect on the vibrational frequency in order to assign to the intermolecular rotational vibrations about the *x*, *y*, and *z* axes.

Experimental

Material. Stilbene-d_0 obtained from Tokyo Kasei Organic Chemicals was purified by zone refining of about 100 passages. Stilbene-d_{12} of 99.7% purity, obtained from CDN Isotopes, was used without further purification. Samples were powdered as fine as possible with a mortar and pestle.

Optical Measurement. The Raman spectra of stilbene-d_0 and -d_{12} crystals due to the inter- and intramolecular vibrations were observed with JOBIN YVON T64000-FU Laser Raman Spectrophotometer at various pressures from 0.1 MPa (1 atm) to about 6 GPa at 298 K. The method of observation of the Raman spectra is exactly the same as described previously.[14,15] A diamond anvil cell obtained from Toshiba Tungaloy Co. was used for measurements of the Raman spectra at high pressures. The powder sample

Published on the web March 12, 2004; DOI 10.1246/bcsj.77.477

and ruby chips suspended in cedar-wood oil were held in a hole made in the center of the stainless-steel gasket. The gasket was placed between the culets of two opposed diamond anvils, and pressure was generated by turning the driving screw attached to the plate which supports the diamond anvils. The pressure was applied by steps of 0.2 GPa from 0.1 MPa to 6 GPa and a series of measurements were made twice to confirm the reproducibility of the observed results. The same series of measurements were also made using nujol as a suspension oil. The pressure inside the gasket hole was measured by the wavelength shift of the R_1 fluorescence line at 694.2 nm emitted from ruby chips, using the equation proposed by Mao et al.[16] The pressure inside the hole was confirmed to be hydrostatic by observing the shapes of the R_1 and R_2 (692.7 nm) fluorescence lines emitted from ruby. The Raman spectra of stilbene-d_0 and -d_{12} crystals were also observed at various temperatures between 77 and 270 K using a cryostat of OXFORD DN1704. The 514.5 and 488.0 nm beams from an Ar^+ ion laser of Spectra Physics Model 2017-04S were used for excitation.

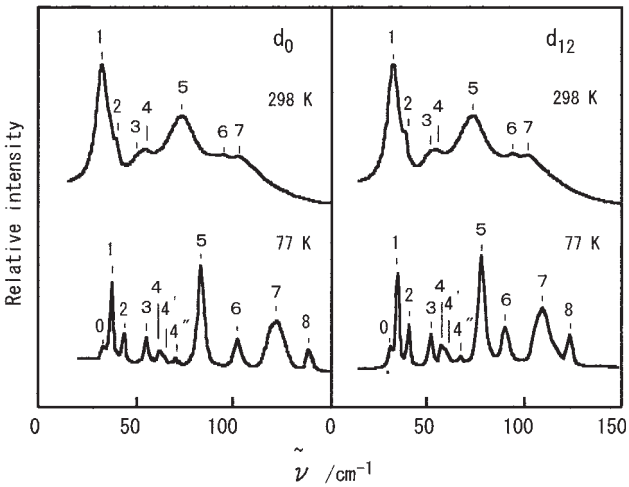

Fig. 1. The Raman spectra of stilbene-d_0 and -d_{12} crystals in the intermolecular vibrational region observed at 298 and 77 K under 0.1 MPa (1 atm).

Results and Discussion

Assignment of the Intermolecular Vibrations. The structures of the molecule and unit cell of stilbene belong to the point group C_{2h}, and the four molecules in the unit cell fall into two symmetrically inequivalent pairs. The intermolecular rotational vibrations about the x, y, and z axes are represented by R_x, R_y, and R_z, respectively. Each vibration splits into two vibrational modes, that is, the in-phase and out-of-phase librations about the rotational axis belonging to the symmetry species A_g and B_g, respectively. Hence, the four molecules in the unit cell give twelve rotational intermolecular vibrations, of which six vibrations belong to the A_g and six to the B_g symmetry species. Assignment to the symmetry species for the Raman bands due to these vibrations was made by Bree and Edelson,[6] but they did not give any assignment to the rotational vibrations as regards the axis (x, y, z) about which the molecule librates in the crystal.

The Raman spectra of stilbene-d_0 and -d_{12} crystals in the low-frequency region observed at 298 and 77 K are shown in Fig. 1. Seven bands marked by 1–7 were observed at 298 K and eleven bands marked by 0–8 were observed at 77 K as shown in Fig. 1. The spectral structure observed at 298 K is almost the same as that observed at 77 K except for shifts of the bands and resolution of the bands marked by 0, 4′, and 4″ and the increase of the relative intensity of bands 7 and 8 compared with the other bands at 77 K. The broad band 7 splits into four bands at 77 K, as suggested for stilbene-d_0 crystal by Bree and Edelson.[6] The frequencies of the individual splitting bands were evaluated to be 118 (106), 120 (108), 123 (111), and 128 (115) cm^{-1} at 77 K by the curve-fitting method using the Voight function. The vibrational frequencies outside and inside of the parentheses are referred to as the frequencies for stilbene-d_0 and -d_{12} crystals, respectively.

The observed frequencies of the Raman bands due to the intermolecular vibrations are given in Table 1 together with the

Table 1. Frequencies of the Stilbene-d_0 and -d_{12} Crystals at 298 and 77 K in the Intermolecular Vibrational Region

Band	Stilbene-d_0			Stilbene-d_{12}		R.F[a]		Assignment
	298 K	77 K	4.2 K[b]	298 K	77 K	298 K	77 K	
	$\tilde{\nu}$/cm^{-1}	$\tilde{\nu}$/cm^{-1}	$\tilde{\nu}$/cm^{-1}	$\tilde{\nu}$/cm^{-1}	$\tilde{\nu}$/cm^{-1}			
0		33	34.9		31		1.06	R_z[c] (a_g)[d]
1	34	37	40.5	32	35	1.06	1.06	R_z (b_g)
2	39	43	46.1	38	41	1.03	1.04	R_y (a_g)
3	54	55	58.0	52	53	1.04	1.04	R_y (b_g)
4	58	62	64.7	55	58	1.05	1.06	R_z (b_g)
4′		65	68.1		63		1.03	R_y (a_g)
4″		70	74.0		67		1.04	R_y (b_g)
5	77	83	86.5	72	78	1.07	1.06	R_z (a_g)
6	97	102	105.3	85	90	1.14	1.13	R_x (a_g)
7	108	118	120.7	97	106	1.11	1.11	torsion[e]
		120	123.4		108		1.11	torsion[e]
		123	127.0		111		1.11	torsion[e]
		128	131.5		115		1.11	torsion[e]
8		139	143.9		123		1.13	intramolecular

a) Ratio of frequency of stilbene-d_0 and -d_{12} ($\tilde{\nu}_{d_0}/\tilde{\nu}_{d_{12}}$) b) Taken from Ref. 6. c) R_x, R_y, and R_z correspond to intermolecular rotational vibrations about x, y, z axes, respectively. d) Symmetry species are taken from Ref. 6. e) Assignment to torsion is taken from Ref. 6.

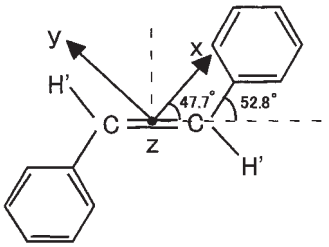

Fig. 2. Principal axes of the moment of inertia of *trans*-stilbene.

Table 2. Moments of Inertia of Stilbene-d_0 and -d_{12}

Axis	x	y	z
I_{d_0} a)	0.31	3.20	3.51
$I_{d_{12}}$ a)	0.38	3.46	3.87
$(I_{d_{12}}/I_{d_0})^{1/2}$	1.11	1.04	1.05

a) Given in 10^{-44} Kg m^2 units. d_0 and d_{12} refer to stilbene-d_0 and -d_{12}, respectively.

isotopic factor of the corresponding bands defined by $\tilde{\nu}_{\text{stilbene-}d_0}/\tilde{\nu}_{\text{stilbene-}d_{12}}$. If the observed low-frequency Raman bands are ascribed to the intermolecular rotational vibrations, the isotopic factor $\tilde{\nu}_{d_0}/\tilde{\nu}_{d_{12}}$ is to be equal to the value of $(I_{rd_{12}}/I_{rd_0})^{1/2}$, where I_r is the moment of inertia of the molecule about the principal axes r $(= x, y, z)$, as shown in Fig. 2. The values of the moment of inertia of stilbene-d_0 and -d_{12} molecules and the values of $(I_{rd_{12}}/I_{rd_0})^{1/2}$ calculated for the molecular structure at room temperature[1] are given in Table 2. The values of the moment of inertia are ranged in the order of $I_x < I_y < I_z$, and the calculated values of $(I_{rd_{12}}/I_{rd_0})^{1/2}$ are 1.11, 1.04, and 1.05 about the x, y, and z axes, respectively. By comparing the isotopic factor of the vibrational frequencies given in Table 1 with the values of $(I_{rd_{12}}/I_{rd_0})^{1/2}$ given in Table 2, the bands 1, 2, 3, 4, 5, and 6 can be assigned to the $R_z(b_g)$, $R_y(a_g)$, $R_y(b_g)$, $R_z(b_g)$, $R_z(a_g)$, and $R_x(a_g)$ vibrations, respectively, where R_x, R_y, and R_z refer to the intermolecular rotational vibrations about x, y, and z axes given in Fig. 2, respectively. The bands 0, 4′, and 4″ observed at 77 K could be assigned to $R_z(a_g)$, $R_y(a_g)$, and $R_y(b_g)$ vibrations, respectively.

The four bands resolved from band 7 in stilbene-d_{12} crystal were assigned to the overtone vibrations of the intramolecular torsional mode of the two phenyl rings belonging to the symmetry species of b_g as assigned for the four bands resolved from band 7 in stilbene-d_0 crystal.[6] As described later, the intensities of bands 7 and 8 increase with increasing pressure compared with the intensities of bands 1–6. The intramolecular vibrations showed the same behavior of intensity increase as observed for bands 7 and 8 with increasing pressure. These observations indicate that band 8 can be assigned to the intramolecular vibration.

Temperature Effect on the Intermolecular Vibrations. Temperature dependences on frequencies and half-band widths of the Raman bands due to the intermolecular vibrations of stilbene-d_0 and -d_{12} were studied through observation of the low frequency Raman spectra at various temperatures between 77 and 270 K under 0.1 MPa. The half-band widths of the Raman bands were determined by the curve-fitting method using the Gaussian function. The curves of the plots of the obtained half-band widths against temperature (temperature–half band width plots) were essentially the same as those given by Chakrabarti and Misra:[7] that is, two break points were observed in the plots at 105–115 K and 215–225 K.

The plots of the frequency shifts against temperature (temperature–frequency shift plots) measured for bands 1 and 5 are shown in Fig. 3. The frequency shift is defined as $\tilde{\nu}_{TK} - \tilde{\nu}_{298K}$, where $\tilde{\nu}_{TK}$ and $\tilde{\nu}_{298K}$ are the vibrational frequencies observed at T K and 298 K, respectively. The frequencies of the observed Raman bands were calibrated with the plasma lines from an Ar^+ ion laser to obtain precise band frequencies. Changes of the slope of the plot curve were observed at temperatures around 100, 140, and 220 K. The peak at about 100 K and the shoulder at about 220 K could correspond to the break points at 105–115 K and 215–225 K observed in the curve of temperature–half band width plots. Observation of a new peak at about 140 K was confirmed to be real, because of the fact that all the plots measured for bands 1–7 show the peaks at about 140 K. The two peaks observed at 105–115 K and at about 140 K may be assigned to another type of order–disorder phase transition. A very weak peak was observed at about 180 K in

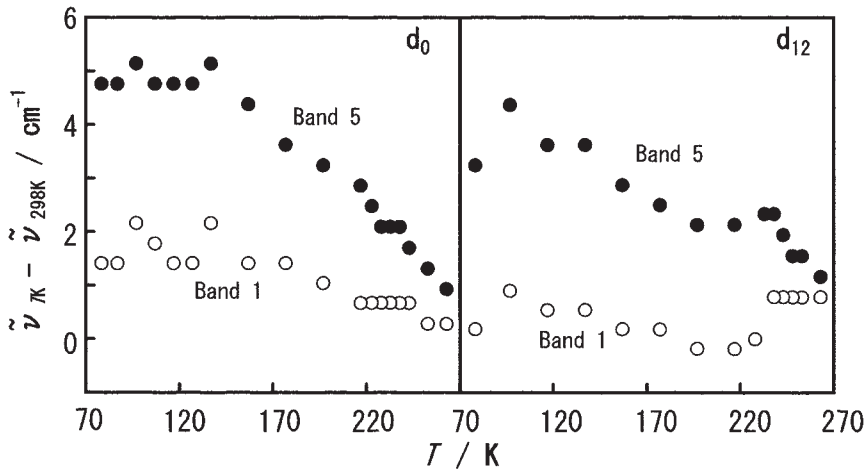

Fig. 3. Temperature–frequency shift plots for the Raman bands of stilbene-d_0 and -d_{12} crystals in the intermolecular vibrational region observed at various temperatures between 77 and 270 K under 0.1 MPa.

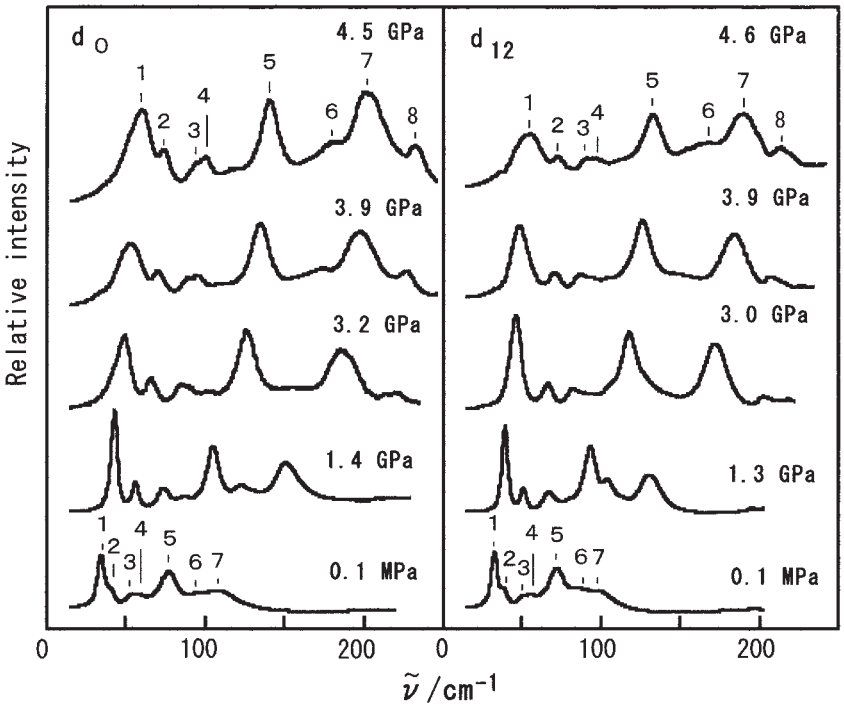

Fig. 4. The Raman spectra of stilbene-d_0 and -d_{12} crystals in the intermolecular vibrational region observed under various pressures at 298 K.

Table 3. Frequencies of Stilbene-d_0 and -d_{12} Crystals under 0.1 MPa and 4.5 GPa in the Intermolecular Vibrational Region

Band	Stillbene-d_0		Stibene-d_{12}	
	0.1 MPa	4.5 MPa	0.1 MPa	4.5 GPa
	$\tilde{\nu}$/cm^{-1}	$\tilde{\nu}$/cm^{-1}	$\tilde{\nu}$/cm^{-1}	$\tilde{\nu}$/cm^{-1}
1	34	59	32	55
2	39	74	38	73
3	54	100	52	97
4	58	95	55	91
5	77	141	72	132
6	97	181	85	167
7[a)]	108	202	97	189

a) Band 7 consists of four bands. See Table 1.

the plot of band 1, but this peak could not be observed in the plots for the other bands. Hence, we could not confirm the existence of the peak at about 170 K assigned to the glass transition by Saito et al.[8]

Pressure Effect on the Intermolecular Vibrations. The Raman spectra of stilbene-d_0 and -d_{12} crystals observed under various pressures in the intermolecular vibrational region are shown in Fig. 4. The Raman spectra of stilbene-d_0 and -d_{12} crystals observed at 0.1 MPa consist of seven bands, marked by 1–7 in the figure, while the spectra at high pressure consist of eight bands marked by 1–8. Figure 4 shows that bands 1–8 shift to the higher frequency side and the relative intensity of bands 1–6 becomes weaker compared with bands 7 and 8 with increasing pressure. The frequencies of the Raman bands observed at 0.1 MPa and 4.5 GPa are given in Table 3. Resolution of the broad band 7 into four bands could not be made by the curve-fitting methods because of the excessive diffuseness of the band.

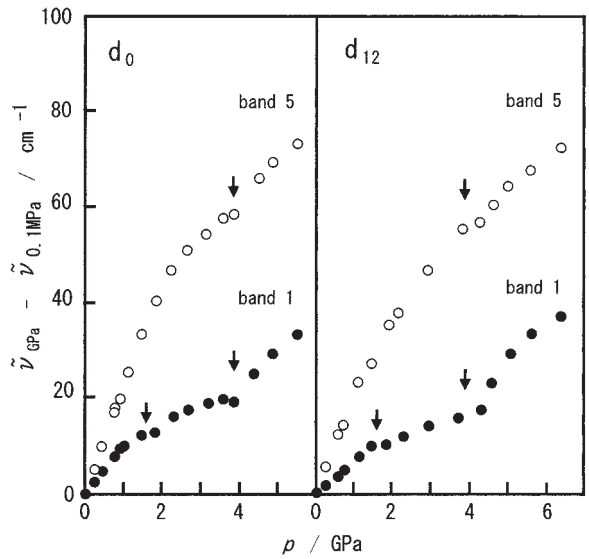

Fig. 5. Pressure–frequency shift plots for the Raman bands of stilbene-d_0 and -d_{12} crystals in the intermolecular vibrational region observed under various pressures at 298 K.

The frequency shift is defined as $\tilde{\nu}_{p\mathrm{GPa}} - \tilde{\nu}_{0.1\mathrm{MPa}}$, where $\tilde{\nu}_{p\mathrm{GPa}}$ and $\tilde{\nu}_{0.1\mathrm{MPa}}$ are the vibrational frequencies observed at pressures of p GPa and 0.1 MPa, respectively. The plots of the observed vibrational frequency shifts against pressure (pressure–frequency shift plots) are shown in Fig. 5. Since strong and sharp Raman bands were selected for the measurements, the precision of the band frequencies was estimated to be less than ± 0.5 cm^{-1} under 0.1 MPa, as considered from

the reproducibility of the calibrated Raman bands. The error in measurement of band frequencies was estimated to be less than ± 1.5 cm^{-1} at 4 GPa.

As can be seen in Fig. 5, the temperature–frequency shift plot for the band 1 shows two shallow and distinct dents at pressure around 1.5–2 and 4 GPa, respectively. The frequency shift increases continuously up to 1.5 GPa, becomes almost constant up to 2 GPa, increases continuously again from 2 to 4 GPa, and then increases steeply from 4 GPa with increasing pressure. The frequency shift of band 5 increases continuously with increasing pressure up to 4 GPa, where a shallow dent was detected; the frequency shift increases continuously again with increasing pressure up to 5.5 GPa. The behavior of variations of the frequency shifts at pressure regions 1.5–2 GPa and 4 GPa and the fact that no clear change of the spectral structure was observed at the pressures from 0.1 MPa to 5.5 GPa will be discussed later, together with the results obtained for the intramolecular vibrations. The Raman bands due to the intermolecular vibrations become diffuse with increasing pressure and thus the half-band width could not be determined through the analysis of the band shapes by the curve fitting method.

Pressure Effect on the Intramolecular Vibrations. The Raman spectra of stilbene-d_0 and -d_{12} crystals in the intramolecular vibrational region are given in Fig. 6, where the vibrational assignments given by Meíc and Güsten[10] are shown. The spectral structure observed under various pressures is essentially the same as that observed at 0.1 MPa,[10] except for the blue shift of the bands and the increase of the half-band width with increasing pressure, as can be seen in molecular crystals.[17,18]

Study of the pressure effect on the vibrational frequency was made for the five strong and well-resolved bands under high pressure. The five bands were observed at 997, 1327, 1193, 1595, and 1640 cm^{-1} under 0.1 MPa for stilbene-d_0.[10] These bands were assigned to the ν_{12} (ring deformation), H′ bending (H′ is ethylenic H atom), C–ϕ stretching (ϕ refers to phenyl ring), ν_{8a} (ring deformation), and ethylenic C=C stretching vibrations, respectively.[10] The bands observed at 956, 1016, 1151, 1554, and 1594 cm^{-1} under 0.1 MPa for stilbene-d_{12} were assigned to the ν_{12}, D′ bending (D′ is ethylenic D atom), C–ϕ stretching, ν_{8a}, and ethylenic C=C stretching vibrations, respectively. The frequencies observed at 0.1 MPa and 4.5 GPa are given in Table 4.

The pressure–frequency shift plots for the bands due to these vibrations are shown in Fig. 7. The band due to the H′ bending vibration of stilbene-d_0 was not detected because of overlapping with the strong diamond band at 1333 cm^{-1} with increasing pressure. Figure 7 shows that (1) the frequency shifts increase monotonously with increasing pressure up to 1.5 GPa at the rate of 2–10 cm^{-1}/GPa, (2) the frequency shifts decrease very slightly (or stay almost constant) with increasing pressure

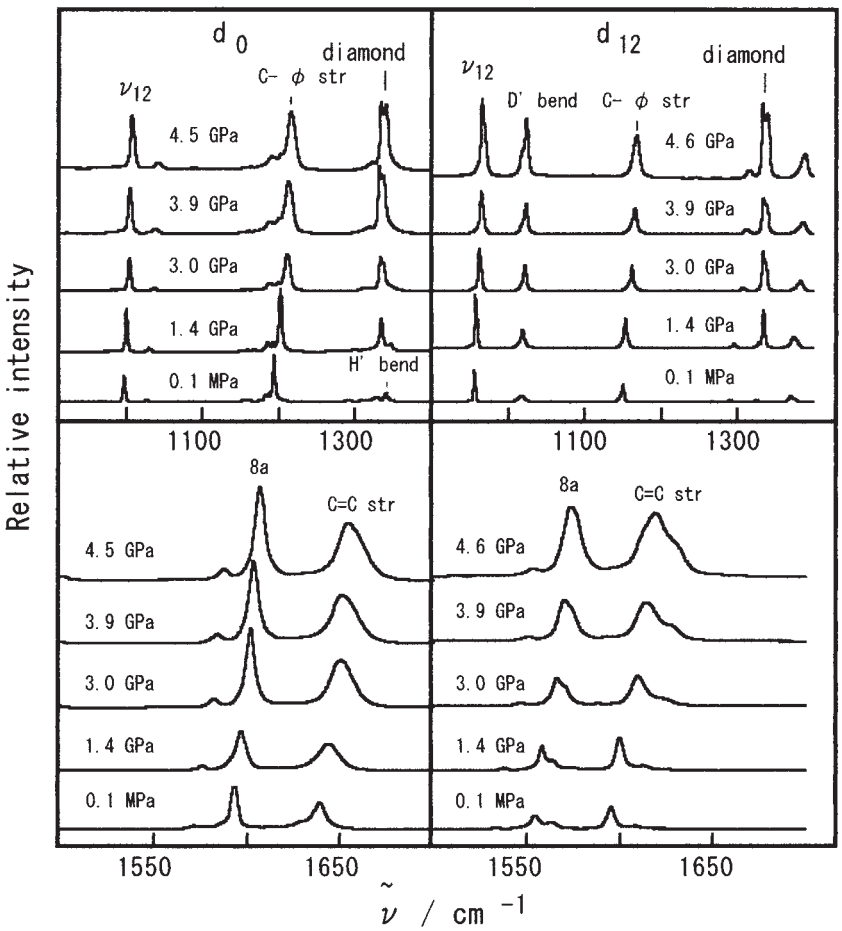

Fig. 6. The Raman spectra of stilbene-d_0 and -d_{12} crystals in the intramolecular vibrational region observed at various pressures at 298 K.

Table 4. Frequencies of Stilbene-d_0 and -d_{12} under 0.1 MPa and 4.5 GPa in the Intramolecular Vibrational Region

Vibrational mode	Stilbene-d_0		Stilbene-d_{12}	
	0.1 MPa	4.5 GPa	0.1 MPa	4.5 GPa
	$\tilde{\nu}$/cm^{-1}	$\tilde{\nu}$/cm^{-1}	$\tilde{\nu}$/cm^{-1}	$\tilde{\nu}$/cm^{-1}
ν_{12}	997	1010	956	965
H′ bend[a)]	1327		1016	1025
C–ϕ str.	1193	1218	1151	1169
ν_{8a}	1595	1611	1554	1572
C=C str.	1640	1658	1594	1617

a) H is replaced by D in stilbene-d_{12}.

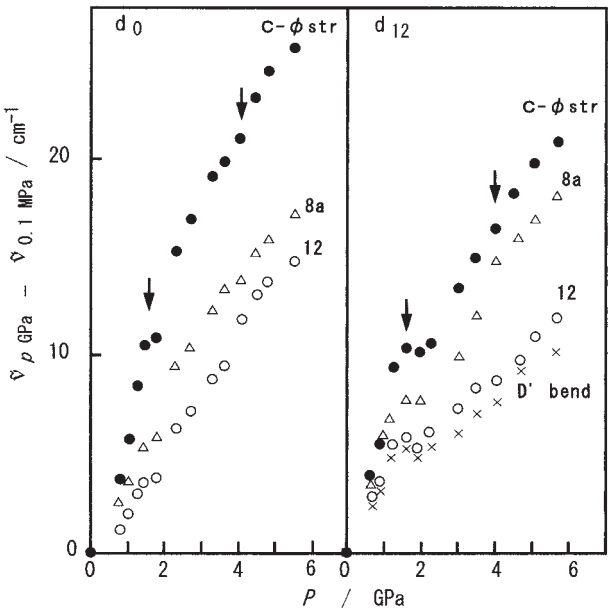

Fig. 7. Pressure–frequency shift plots for stilbene-d_0 and -d_{12} crystals in the intramolecular vibrational region observed at various pressures at 298 K.

from 1.5 GPa to 2 GPa, and (3) the frequency shifts increase again monotonously with increasing pressure from 2 and 5.5 GPa at the rate of 2–10 cm^{-1}/GPa, depending on the vibrational modes. Careful observation of the plots indicates that a quite shallow dent exists at 4 GPa. The variational behavior of the frequency shift at pressure region 1.5–2 GPa was observed more prominently for stilbene-d_{12} crystal than for stilbene-d_0 crystal. The observation of the changes of frequency shifts at 1.5–2 GPa and 4–5.5 GPa is in accord with the observed result for the intermolecular vibrations.

The pressure–half band width plots for the ν_{12}, C–ϕ stretching, and ν_{8a} vibrations are shown in Fig. 8. This shows that (1) the slopes of the curves of the pressure–band width plots for the bands ν_{12}, C–ϕ stretching, and ν_{8a} vibrations increase slightly (or almost constantly) from 0.1 MPa to 1.5 GPa, (2) the slopes decrease very slightly (or stay almost constant) from 1.5 to 2 GPa, (3) the slopes increase slightly from 2 to 4 GPa, and (4) the slopes increase greatly from 4 to 5.5 GPa.

The pressure-induced frequency shift and variation of the half-band width are related to the change of the intermolecular interactions.[14,15,17,18] If a first-order phase transition takes place, the crystal structure deforms abruptly and discontinuous changes of the frequency shift and band width are expected to be observed at the pressure where the phase transition is induced. On the other hand, if a second-order phase transition takes place, the crystal structure deforms continuously over the pressure regions, where the phase transition is induced, and inflectional variations of the slopes of the pressure–frequency shift plots and pressure–band width plots are expected to be observed.

The observed changes of the pressure–frequency shift plots and pressure–band width plots for the inter- and intramolecular vibrations for stilbene-d_0 and -d_{12} crystals indicate that the intermolecular interactions change at the pressure regions 1.5–2 GPa and 4 GPa: that is, the phase transitions take place at these pressure regions: 1.5–2 GPa and 4 GPa. The pressure–frequency shift plots and pressure–half band width plots do not show clear discontinuous change but the slopes of both the plots show inflectional variation at these pressure regions: 1.5–2 GPa and 4 GPa. These results indicate that the second-order phase transi-

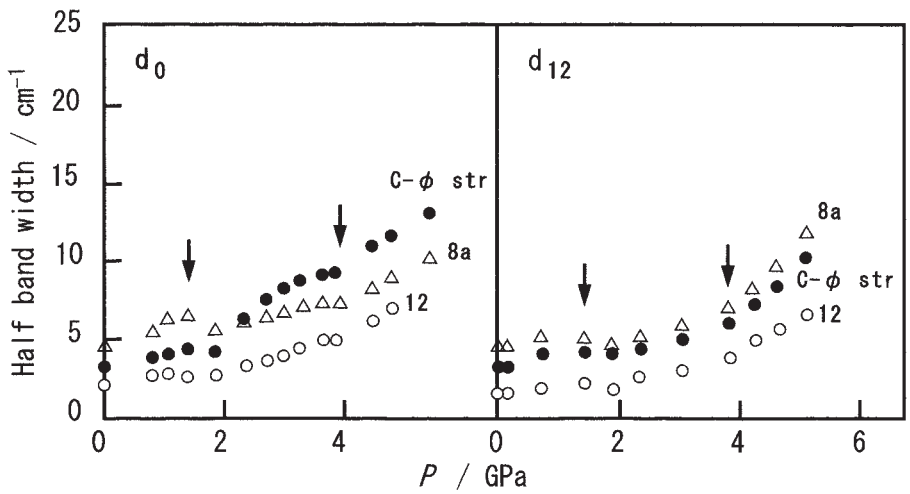

Fig. 8. Pressure–band width plots for stilbene-d_0 and -d_{12} crystals in the intramolecular vibrational region observed at various pressures at 298 K.

tions take place at 1.5–2 GPa and 4 GPa regions in stilbene-d_0 and -d_{12} crystals.

The compression for crystals at the temperature of 77 K under 0.1 MPa approximately corresponds to the pressure of about 1 GPa applied to crystals at room temperature. No changes of the slopes of the pressure–frequency shift plots and pressure–half band width plots for the intra- and intermolecular vibrations at low-pressure region (see Figs. 5, 7, and 8), corresponding to the changes of the slopes of the temperature–frequency shift plots and temperature–half band width plots for the intermolecular vibrations observed at temperature regions 105–115, about 140, and 215–225 K (see Fig. 3), could be observed. The reason for this result may be the fact that the changes of the slopes of the both plots for the pressure dependences are small at these low-pressure regions.

The authors thank the Japan Private School Promotion Foundation for Science Research Promotion Fund.

References

1 C. J. Finder, M. G. Newton, and N. L. Allinger, *Acta Crystallogr.*, **B30**, 411 (1974).

2 A. Hoekstra, P. Meertens, and A. Vos, *Acta Crystallogr.*, **B31**, 2813 (1975).

3 J. A. Bouwstra, A. Schouten, and J. Kroon, *Acta Crystallogr.*, **C40**, 428 (1984).

4 M. Traetteberg, E. B. Frantsen, F. C. Mijlhoff, and A. Hoekstra, *J. Mol. Struct.*, **26**, 57 (1975).

5 M. Edelson and A. Bree, *Chem. Phys. Lett.*, **41**, 562 (1976).

6 A. Bree and M. Edelson, *Chem. Phys.*, **51**, 77 (1980).

7 S. Chakrabarti and T. N. Misra, *Bull. Chem. Soc. Jpn.*, **64**, 2454 (1991).

8 K. Saito, Y. Yamamura, K. Kikuchi, and I. Ikemoto, *J. Phys. Chem. Solids. Jpn.*, **56**, 849 (1995).

9 K. Saito and I. Ikemoto, *Bull. Chem. Soc. Jpn.*, **69**, 909 (1996).

10 Z. Meíc and H. Güsten, *Spectrochim. Acta*, **34**, 101 (1978).

11 A. Warshel, *J. Chem. Phys.*, **62**, 214 (1975).

12 K. Palmö, *Spectrochim. Acta*, **44A**, 341 (1988).

13 H. Watanabe, Y. Okamoto, K. Furuya, A. Sakamoto, and M. Tasumi, *J. Phys. Chem. A*, **106**, 3318 (2002).

14 Y. Towata, Y. Suzuki, Y. Nibu, H. Shimada, and R. Shimada, *Bull. Chem. Soc. Jpn.*, **74**, 1251 (2001).

15 Y. Uchida, C. Okabe, A. Kishi, H. Takeshita, Y. Suzuki, Y. Nibu, H. Shimada, and R. Shimada, *Bull. Chem. Soc. Jpn.*, **75**, 695 (2002).

16 H. K. Mao, P. M. Bell, J. W. Shaner, and D. J. Steinberg, *J. Appl. Phys.*, **49**, 3276 (1978).

17 M. Maehara, H. Kawano, Y. Nibu, H. Shimada, and R. Shimada, *Bull. Chem. Soc. Jpn.*, **68**, 506 (1995).

18 H. Mizobe, H. Shimada, and R. Shimada, *Int. J. Quantum Chem.*, **72**, 287 (1999).